AIAA JOURNAL
Vol. 33, No. 7, July 1995

Energy-Based Dynamic Buckling Estimates for Autonomous Dissipative Systems

C. Gantes* and A. N. Kounadis†
National Technical University of Athens, Athens 10682, Greece

The dynamic buckling global response of a nonlinear, 3-degree-of-freedom dissipative model under a step loading of infinite duration is thoroughly discussed. Geometrically imperfect models with symmetric or antisymmetric imperfections losing their static stability through a limit point and an asymmetric bifurcation point, respectively, are considered. Emphasis is given to the combined effect of nonlinearities (geometric and/or material) and damping. Exact, approximate, and lower/upper bound estimates based on energy criteria for establishing the dynamic buckling response of such autonomous models without solving the highly nonlinear initial-value problem are assessed. The reliability and efficiency of the proposed readily obtained estimates is illustrated via numerical simulation, the accuracy of which is checked using energy balance considerations. Certain interesting byproducts associated with a postlimit point bifurcation and breakdown of the symmetry of deformation are also revealed.

I. Introduction

THE intractability of nonlinear initial-value problems associated with the dynamic buckling response of discrete dissipative/nondissipative autonomous systems still remains a serious computational problem, in spite of the availability of modern, very efficient computational techniques and high-speed computers. This is particularly true when dynamic buckling may occur after a long time or in case of the existence of chaotic-like phenomena due to sensitivity to initial conditions or due to damping. In such cases the numerical algorithms that are employed for the solution of the differential equations of motion may experience convergence difficulties. This work, which is a further extension of previous observations and findings[1–4] related to the problem of nonlinear dynamic buckling of multi-degree-of-freedom (DOF) discrete structural systems, aims at overcoming the aforementioned drawbacks. Indeed, in this analysis very efficient and readily obtained lower/upper bound dynamic buckling estimates in addition to exact ones for the special case of vanishing (but nonzero) damping are established. The lower bound estimates are based on the energy criterion associated with the vanishing of the total potential energy on a certain equilibrium point of the unstable postbuckling path.[2,3,5] A very efficient approximate dynamic buckling estimate based on energy considerations and on Schwarz's and Holder's inequality is recently reported.[7] The reliability and efficiency of all of the preceding dynamic buckling estimates is investigated in using a 3-DOF model subjected to a step load of infinite duration with the aid of numerical simulation and an analytical approximate technique.[8]

II. Mathematical Analysis

Consider a general n-DOF dissipative structural system subjected to a step load λ of infinite duration. The response of the system can be described by the following set of nonlinear ordinary differential equations of motion of Lagrange:

$$\frac{\mathrm{d}}{\mathrm{d}t}\left(\frac{\partial K}{\partial \dot{q}_i}\right) - \frac{\partial K}{\partial q_i} + \frac{\partial V_T}{\partial q_i} + \frac{\partial F}{\partial \dot{q}_i} = 0, \qquad i = 1, \ldots, n \quad (1)$$

where q_i and $\dot{q}_i$ are the generalized coordinates, whereas the dots denote differentiation with respect to time t; $K = 0.5 \cdot \dot{\boldsymbol{q}}^T \cdot \boldsymbol{a} \cdot \dot{\boldsymbol{q}}$ is the positive definite function of the total kinetic energy with corresponding matrix $\boldsymbol{a}$ having nondiagonal elements $a_{ij} = a_{ij}(q_1, \ldots, q_n)$, where $\boldsymbol{q}$ is a state vector with its transpose $\boldsymbol{q}^T$ having components q_i; $V_T = V_T(q_1, \ldots, q_n, \lambda)$ is the total potential energy, which is assumed to be a nonlinear function of q_i and a linear function of the loading parameter λ; $F = 0.5 \cdot \dot{\boldsymbol{q}}^T \cdot \boldsymbol{c} \cdot \dot{\boldsymbol{q}}$ is the nonnegative definite, viscous dissipation function of Rayleigh, and $\boldsymbol{c}$ is the corresponding non-negative definite damping matrix with damping coefficients c_{ij}. The loading λ is considered as the main control parameter for the occurrence of static and dynamic bifurcations. It is also assumed that this system under the same loading λ applied statically exhibits a limit point instability. This analysis is applied to discrete systems or to continuous systems which have been discretized by some approximation technique. It is also applicable after slight modification to impulse or impact load.[9]

Dynamic buckling (escaped motion) of a structural system is defined as the state at which an infinitesimal variation of the applied load results in a response associated with large displacements. The minimum load corresponding to that state is defined as the dynamic buckling load λ_{DD}.

The exact value of the dynamic buckling load λ_{DD} of a structural system under the aforementioned types of loading can be obtained numerically by integrating the equations of motion (1) subject to given initial conditions. However, such numerical solutions very often experience computational difficulties, especially when dynamic buckling may occur after a long time or in the presence of chaotic-like phenomena due to sensitivity to initial conditions or due to sensitivity to damping. Therefore, it is highly desirable to supplement numerical simulation by other solutions such as approximate or lower/upper bound estimates for the dynamic buckling load. Such estimates not only help us as monitor of the accuracy of the numerical algorithms but also provide fast and inexpensive approximations that can be very useful for structural design purposes.

The limit point load λ_s is an upper bound of the dynamic buckling load λ_{DD} as has been demonstrated both for systems subjected to step loads of infinite duration[2,3] or under impact load[9]:

$$\lambda_{DD} < \lambda_s \quad (2)$$

Lower bound dynamic buckling estimates can be obtained if one resorts to energy considerations. For a system initially ($t = 0$) at rest, the total energy E, including the dissipation of energy, can be expressed in dimensionless form as

$$E = K + V_T + 2 \cdot \int_0^\tau F \cdot \mathrm{d}\tau = K^0 \quad (3)$$

where K^0 is the initial kinetic energy at time $t = 0$ that can be evaluated by means of the known initial conditions. From Eq. (3) it can be easily observed that throughout motion the quantity $(V_T - K^0)$ is

Received Jan. 12, 1984; revision received Sept. 15, 1994; accepted for publication Sept. 16, 1994.

*Lecturer, Structural Analysis and Steel Bridges.
†Professor and Director, Structural Analysis and Steel Bridges. Senior Member AIAA.

negative definite. This is also true at the instant of occurrence of dynamic buckling (escaped motion). Taking into account that dynamic buckling takes place via a saddle point corresponding to $\lambda_{DD} < \lambda_s$ the kinetic energy at that time becomes zero. Hence, Eq. (3) yields

$$V_T = -2 \cdot \int_0^\tau F \cdot d\tau + K^0 \tag{4}$$

If the system is initially at rest Eq. (4) becomes

$$V_T = -2 \cdot \int_0^\tau F \cdot d\tau \tag{5}$$

This condition can only be valid if

$$V_T(q_i^s;\ \lambda) \le -2 \cdot \int_0^\tau F \cdot d\tau, \qquad i = 1, \ldots, n \tag{6}$$

where q_i^s are the values of the displacements at the limit point. From Eq. (6) one can obtain for the case of vanishing but nonzero damping ($c_{ij} \to 0,\ i,j = 1, \ldots, n$)

$$V_T = 0 \tag{7}$$

Equation (7) combined with the static equilibrium equations

$$\frac{\partial V_T}{\partial q_i} = 0, \qquad i = 1, \ldots, n \tag{8}$$

yield the exact dynamic buckling load $\tilde{\lambda}_D$ for vanishing but nonzero damping. It should be noted that this load can be obtained without need to integrate the differential equations of motion (1). It can further be observed that when the amount of damping decreases $\tilde{\lambda}_D$ approaches the accurate dynamic buckling load λ_{DD}. Hence, $\tilde{\lambda}_D$ is a lower bound estimate of λ_{DD}, that is,

$$\tilde{\lambda}_D < \lambda_{DD} \tag{9}$$

Combining relations (2) and (9) one can obtain

$$\tilde{\lambda}_D < \lambda_{DD} < \lambda_s \tag{10}$$

This result can be extended to the case of undamped structural systems under dynamic load. This is a rather unrealistic case since damping is always present in real structural systems. Denoting by λ_D the exact value of the dynamic buckling load of the undamped system, one can get[2,3]

$$\tilde{\lambda}_D < \lambda_D < \lambda_{DD} < \lambda_s \tag{11}$$

In the case of 1-DOF systems this result is slightly modified:

$$\tilde{\lambda}_D \equiv \lambda_D < \lambda_{DD} < \lambda_s \tag{12}$$

Consider now Eq. (5). Since a closed-form evaluation of the integral in the right-hand side is, in general, impossible one has to resort to upper or lower bound estimates of it. This can be achieved by using the inequality[9] of Schwarz and Holder for any function $\dot{X}(t)$ that is integrable in the interval $[\tau_0, \tau]$:

$$|X(\tau) - X(\tau_0)|^2 = \left| \int_{\tau_0}^\tau \dot{X}(t)\, dt \right|^2 \le (\tau - \tau_0) \cdot \int_{\tau_0}^\tau |\dot{X}(t)|^2\, dt \tag{13}$$

If $\boldsymbol{X}(t) = [X_1(t), \ldots, X_n(t)]^T$ inequality (13) becomes

$$\bar{\boldsymbol{X}}^T \cdot \bar{\boldsymbol{X}} = \sum_{i=1}^n \left| \int_{\tau_0}^\tau \dot{X}_i(t)\, dt \right|^2 \le (\tau - \tau_0) \cdot \int_{\tau_0}^\tau |\dot{\boldsymbol{X}}^T \cdot \dot{\boldsymbol{X}}|\, dt \tag{14}$$

where $\bar{\boldsymbol{X}} = \boldsymbol{X}(\tau) - \boldsymbol{X}(\tau_0)$.

Since the elements of the non-negative damping matrix $[c_{ij}]$ are scalar quantities using relation (14) we obtain

$$\frac{c_{ij}}{\tau} \cdot \bar{q}_i \cdot \bar{q}_j \le \int_0^\tau c_{ij} \cdot \dot{q}_i \cdot \dot{q}_j \cdot dt, \qquad i,j = 1, \ldots, n \tag{15}$$

where $\bar{q}_i = q_i(\tau) - q_i^0$. Obviously, the Einstein summation convention has been employed.

Then, Eq. (6) with the aid of inequality (15) can be written as follows:

$$V_T \le -(c_{ij}/\tau) \cdot \bar{q}_i \cdot \bar{q}_j, \qquad i,j = 1, \ldots, n \tag{16}$$

The solution of the combined Eq. (16) and (8) provides another approximate estimate of the dynamic buckling load for the dissipative system. Such a solution is acceptable only when it corresponds to a saddle point of the unstable postbuckling equilibrium path. The approximate dynamic buckling load $\bar{\lambda}_{DD}$ obtained in this way is a lower bound estimate of the exact load λ_{DD} provided that the length of time τ (from the onset of loading until the instant of dynamic buckling) is known. However, this is never the case. Hence, the half-period $\bar{\tau} = \pi/\omega_0$ of the linearized system can be used as an approximate value of τ, where ω_0 is the fundamental frequency. It should be noted that $\bar{\tau}$ is a much smaller than τ, especially when the number of degrees of freedom of the system increases and the amount of damping decreases. Therefore, under these conditions the load $\bar{\lambda}_{DD}$ obtained from Eqs. (16) and (8) using $\bar{\tau}$ is an approximate dynamic buckling estimates which is acceptable only when

$$\tilde{\lambda}_D < \bar{\lambda}_{DD} < \lambda_s \tag{17}$$

Hence, Eqs. (11) and (12) can be combined with Eq. (17) and are finally written as

$$\tilde{\lambda}_D \approx \lambda_D < \lambda_{DD} \approx \bar{\lambda}_{DD} < \lambda_s \tag{18a}$$

$$\tilde{\lambda}_D \equiv \lambda_D < \lambda_{DD} \approx \bar{\lambda}_{DD} < \lambda_s \tag{18b}$$

for multi- and single-DOF systems, respectively.

III. Description of Structural System

Consider the nonlinear elastic model of cubic type shown in Fig. 1, which consists of four pin-jointed rigid bars of equal length L. Three concentrated masses, m_1, m_2, and m_3 attached at the pinned connections are supported by three vertical nonlinear springs that exhibit a softening behavior described by the equations

$$F_i = k_i \cdot y_i - a_i \cdot k_i \cdot y_i^3, \qquad i = 1, 2, 3 \tag{19}$$

where k_i and a_i are the linear and nonlinear spring constants whereas y_i are the respective displacements. The three springs are also linear viscoelastic in the vertical direction with corresponding coefficients c_1, c_2, and c_3.

The model at its right end is subjected to a step load Λ of infinite duration. The deformed configuration is described by the angles ϑ_1, ϑ_2, and ϑ_3, whereas the undeformed configuration is defined by the initial angle imperfections denoted by ε_1, ε_2, and ε_3.

The kinetic energy K, the strain energy U, the potential energy of the external loading Ω, and the Rayleigh dissipation function F are given by

$$\begin{aligned} K = \tfrac{1}{2} L^2 \{ & (m_1 + m_2 + m_3)\dot{\vartheta}_1^2 + (m_2 + m_3)\dot{\vartheta}_2^2 + m_3 \cdot \dot{\vartheta}_3^2 \\ & + 2(m_2 + m_3)\dot{\vartheta}_1 \cdot \dot{\vartheta}_2 \cdot \cos(\vartheta_1 - \vartheta_2) - 2 \cdot m_3 \cdot \dot{\vartheta}_1 \cdot \dot{\vartheta}_3 \\ & \cdot \cos(\vartheta_1 + \vartheta_3) - 2 \cdot m_3 \cdot \dot{\vartheta}_2 \cdot \dot{\vartheta}_3 \cdot \cos(\vartheta_2 + \vartheta_3) \} \end{aligned} \tag{20}$$

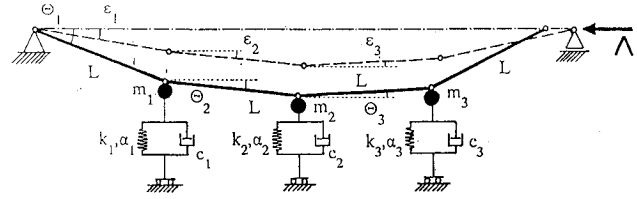

Fig. 1 Geometry of an imperfect 3-DOF system composed of four rigid links interconnected by three frictionless hinges carrying corresponding concentrated masses supported by three nonlinear and viscoelastic springs.

$$U = \tfrac{1}{2}k_1 \cdot L^2(\sin\vartheta_1 - \sin\varepsilon_1)^2 - \tfrac{1}{4}a_1 \cdot k_1 \cdot L^4(\sin\vartheta_1 - \sin\varepsilon_1)^4 + \tfrac{1}{2}k_2 \cdot L^2(\sin\vartheta_1 + \sin\vartheta_2 - \sin\varepsilon_1 - \sin\varepsilon_2)^2 - \tfrac{1}{4}a_2 \cdot k_2 \cdot L^4(\sin\vartheta_1 + \sin\vartheta_2 - \sin\varepsilon_1 - \sin\varepsilon_2)^4 + \tfrac{1}{2}k_3 \cdot L^2(\sin\vartheta_1 + \sin\vartheta_2 - \sin\vartheta_3 - \sin\varepsilon_1 - \sin\varepsilon_2 + \sin\varepsilon_3)^2 - \tfrac{1}{4}a_3 \cdot k_3 \cdot L^4(\sin\vartheta_1 + \sin\vartheta_2 - \sin\vartheta_3 - \sin\varepsilon_1 - \sin\varepsilon_2 + \sin\varepsilon_3)^4 \quad (21)$$

$$\Omega = \Lambda \cdot L\Big\{\sqrt{1 - (\sin\varepsilon_1 + \sin\varepsilon_2 - \sin\varepsilon_3)^2} - \sqrt{1 - (\sin\vartheta_1 + \sin\vartheta_2 - \sin\vartheta_3)^2} + \cos\varepsilon_1 + \cos\varepsilon_2 + \cos\varepsilon_3 - \cos\vartheta_1 - \cos\vartheta_2 + \cos\vartheta_3\Big\} \quad (22)$$

$$F = (L^2/2)\big\{(c_{11} + c_{22} + c_{33} + 2 \cdot c_{12} + 2 \cdot c_{23} + 2 \cdot c_{13})\dot{\vartheta}_1^2 \cdot \cos^2\vartheta_1 + (c_{22} + c_{33} + 2 \cdot c_{23})\dot{\vartheta}_2^2 \cdot \cos^2\vartheta_2 + c_{33} \cdot \dot{\vartheta}_3^2 \cdot \cos^2\vartheta_3 + 2(c_{22} + c_{33} + c_{12} + 2 \cdot c_{23} + c_{13})\dot{\vartheta}_1 \cdot \dot{\vartheta}_2 \cdot \cos\vartheta_1 \cdot \cos\vartheta_2 - 2(c_{33} + c_{23})\dot{\vartheta}_2 \cdot \dot{\vartheta}_3 \cdot \cos\vartheta_2 \cdot \cos\vartheta_3 - 2(c_{33} + c_{23} + c_{13})\dot{\vartheta}_1 \cdot \dot{\vartheta}_3 \cdot \cos\vartheta_1 \cdot \cos\vartheta_3\big\} \quad (23)$$

where c_{ij} are the damping coefficients of the non-negative Rayleigh dissipative matrix. For the model under consideration $c_{11} = c_1$, $c_{22} = c_2$, $c_{33} = c_3$, whereas $c_{12} = c_{23} = c_{13} = 0$. For the sake of simplicity the following assumptions were also made:

$$k_1 = k_2 = k_3 = k,\ a_1 = a_2 = a_3 = a/L^2$$

$$m_1 = m_2 = m_3 = m$$

Lagrange equations of motion are given by Eq. (1) where $V_T = U + \Omega$.

To nondimensionalize the problem we can introduce the transformation variables

$$\tau = t\sqrt{\frac{k}{m}}, \qquad \theta_i(\tau) = \vartheta_i(t), \qquad \hat{c}_i = \frac{c_{ii}}{\sqrt{k \cdot m}}$$

$$\lambda_c = \frac{k \cdot L}{3.4142135}, \qquad \lambda = \frac{\Lambda}{3.4142135} \quad (24)$$

The scaling factor 3.4142135 results from the relation[10]

$$\lambda_c = \frac{k \cdot L}{4 \cdot \sin^2[n \cdot \pi/2 \cdot (n+1)]}, \qquad n = 1, 2, \ldots \quad (25)$$

for $n = 1$.

Then, the equations of motion are written as follows:

$$3 \cdot \ddot{\theta}_1 + 2 \cdot \cos(\theta_1 - \theta_2) \cdot \ddot{\theta}_2 - \cos(\theta_1 + \theta_3) \cdot \ddot{\theta}_3 + (\hat{c}_1 + \hat{c}_2 + \hat{c}_3) \cdot \cos^2\theta_1 \cdot \dot{\theta}_1 + (\hat{c}_2 + \hat{c}_3) \cdot \cos\theta_1 \cdot \cos\theta_2 \cdot \dot{\theta}_2 - \hat{c}_3 \cdot \cos\theta_1 \cdot \cos\theta_3 \cdot \dot{\theta}_3 + 2 \cdot \sin(\theta_1 - \theta_2) \cdot \dot{\theta}_2^2 + \sin(\theta_1 + \theta_3) \cdot \dot{\theta}_3^2 + \frac{\partial V}{\partial \theta_1} = 0 \quad (26)$$

$$2 \cdot \cos(\theta_1 - \theta_2) \cdot \ddot{\theta}_1 + 2 \cdot \ddot{\theta}_2 - \cos(\theta_2 + \theta_3) \cdot \ddot{\theta}_3 + (\hat{c}_2 + \hat{c}_3) \cdot \cos\theta_1 \cdot \cos\theta_2 \cdot \dot{\theta}_1 + (\hat{c}_2 + \hat{c}_3) \cdot \cos^2\theta_2 \cdot \dot{\theta}_2 - \hat{c}_3 \cdot \cos\theta_2 \cdot \cos\theta_3 \cdot \dot{\theta}_3 - 2 \cdot \sin(\theta_1 - \theta_2) \cdot \dot{\theta}_1^2 + \sin(\theta_2 + \theta_3) \cdot \dot{\theta}_3^2 + \frac{\partial V}{\partial \theta_2} = 0 \quad (27)$$

$$-\cos(\theta_1 + \theta_3) \cdot \ddot{\theta}_1 + -\cos(\theta_2 + \theta_3) \cdot \ddot{\theta}_2 + \ddot{\theta}_3 - \hat{c}_3 \cdot \big(\cos\theta_1 \cdot \cos\theta_3 \cdot \dot{\theta}_1 + \cos\theta_2 \cdot \cos\theta_3 \cdot \dot{\theta}_2 - \cos^2\theta_3 \cdot \dot{\theta}_3\big) + \sin(\theta_1 + \theta_3) \cdot \dot{\theta}_1^2 + \sin(\theta_2 + \theta_3) \cdot \dot{\theta}_2^2 + \frac{\partial V}{\partial \theta_3} = 0 \quad (28)$$

where

$$\frac{\partial V}{\partial \theta_1} = \cos\theta_1 \cdot \Big\{(\sin\theta_1 - \sin\varepsilon_1) \cdot \big[1 - a \cdot (\sin\theta_1 - \sin\varepsilon_1)^2\big] + (\sin\theta_1 + \sin\theta_2 - \sin\varepsilon_1 - \sin\varepsilon_2) \cdot \big[1 - a \cdot (\sin\theta_1 + \sin\theta_2 - \sin\varepsilon_1 - \sin\varepsilon_2)^2\big] + (\sin\theta_1 + \sin\theta_2 - \sin\theta_3 - \sin\varepsilon_1 - \sin\varepsilon_2 + \sin\varepsilon_3) \cdot \big[1 - a \cdot (\sin\theta_1 + \sin\theta_2 - \sin\theta_3 - \sin\varepsilon_1 - \sin\varepsilon_2 + \sin\varepsilon_3)^2\big]\Big\} - \frac{\lambda}{\lambda_c} \cdot \left\{\frac{(\sin\theta_1 + \sin\theta_2 - \sin\theta_3) \cdot \cos\theta_1}{\sqrt{1 - (\sin\theta_1 + \sin\theta_2 - \sin\theta_3)^2}} + \sin\theta_1\right\} \quad (29)$$

$$\frac{\partial V}{\partial \theta_2} = \cos\theta_2 \cdot \Big\{(\sin\theta_1 + \sin\theta_2 - \sin\varepsilon_1 - \sin\varepsilon_2) \cdot \big[1 - a \cdot (\sin\theta_1 + \sin\theta_2 - \sin\varepsilon_1 - \sin\varepsilon_2)^2\big] + (\sin\theta_1 + \sin\theta_2 - \sin\theta_3 - \sin\varepsilon_1 - \sin\varepsilon_2 + \sin\varepsilon_3) \cdot \big[1 - a \cdot (\sin\theta_1 + \sin\theta_2 - \sin\theta_3 - \sin\varepsilon_1 - \sin\varepsilon_2 + \sin\varepsilon_3)^2\big]\Big\} - \frac{\lambda}{\lambda_c} \cdot \left\{\frac{(\sin\theta_1 + \sin\theta_2 - \sin\theta_3) \cdot \cos\theta_2}{\sqrt{1 - (\sin\theta_1 + \sin\theta_2 - \sin\theta_3)^2}} + \sin\theta_2\right\} \quad (30)$$

$$\frac{\partial V}{\partial \theta_3} = -\cos\theta_3 \cdot \Big\{(\sin\theta_1 + \sin\theta_2 - \sin\theta_3 - \sin\varepsilon_1 - \sin\varepsilon_2 + \sin\varepsilon_3) \cdot \big[1 - a \cdot (\sin\theta_1 + \sin\theta_2 - \sin\theta_3 - \sin\varepsilon_1 - \sin\varepsilon_2 + \sin\varepsilon_3)^2\big]\Big\} - \frac{\lambda}{\lambda_c} \cdot \left\{\frac{(\sin\theta_1 + \sin\theta_2 - \sin\theta_3) \cdot \cos\theta_3}{\sqrt{1 - (\sin\theta_1 + \sin\theta_2 - \sin\theta_3)^2}} + \sin\theta_3\right\} \quad (31)$$

In the static case $\dot{\theta}_i = \ddot{\theta}_i = 0$, $(i = 1, 2, 3)$, and the model is described by the following nonlinear equilibrium equations:

$$\frac{\partial V}{\partial \theta_1} = \frac{\partial V}{\partial \theta_2} = \frac{\partial V}{\partial \theta_3} = 0 \quad (32)$$

Equilibrium paths can be obtained by step increasing one parameter, whereas the other parameters are kept constant.

A solution to the dynamic problem is achieved by solving the system of Eqs. (26–28) for $\ddot{\theta}_1, \ddot{\theta}_2$, and $\ddot{\theta}_3$ and then applying a fourth-order Runge–Kutta numerical scheme. These processes can encounter computational difficulties, especially when dynamic buckling may occur after a long time, or in case of chaotic-like phenomena due to sensitivity to initial conditions or due to damping. To alleviate such problems numerical simulation has been supplemented by the approximate or lower and upper bound estimates for the dynamic buckling load that have been presented in the previous paragraph. Such estimates not only help us as monitor of the accuracy of the numerical algorithms, but also provide fast and inexpensive approximations that can be very useful for structural design purposes. Note also that the energy balance in Eq. (3) or (5) can be used for checking the accuracy of numerical solutions.

The fundamental period of the 3-DOF cantilever system of Fig. 1 which is needed to compute the approximate load $\bar{\lambda}_{DD}$ can be approximated by linearizing the equations of motion (26–28). Linearization is performed by neglecting quadratic and higher order terms as well as the effects of damping and initial imperfections,

and by assuming small angles and, hence, setting $\sin\theta \approx \theta$, $\cos\theta \approx$. Then, the following linearized equations of motion are obtained:

$$3\cdot\ddot{\theta}_1 + \left(3 - 2\frac{\bar{\lambda}}{\lambda_c}\right)\theta_1 + 2\cdot\ddot{\theta}_2 + \left(2 - \frac{\bar{\lambda}}{\lambda_c}\right)\theta_2 - \ddot{\theta}_3 - \left(1 - \frac{\bar{\lambda}}{\lambda_c}\right)\theta_3 = 0 \tag{33}$$

$$2\cdot\ddot{\theta}_1 + \left(2 - \frac{\bar{\lambda}}{\lambda_c}\right)\theta_1 + 2\cdot\ddot{\theta}_2 + \left(2 - 2\frac{\bar{\lambda}}{\lambda_c}\right)\theta_2 - \ddot{\theta}_3 - \left(1 - \frac{\bar{\lambda}}{\lambda_c}\right)\theta_3 = 0 \tag{34}$$

$$-\ddot{\theta}_1 - \left(1 - \frac{\bar{\lambda}}{\lambda_c}\right)\theta_1 - \ddot{\theta}_2 - \left(1 - \frac{\bar{\lambda}}{\lambda_c}\right)\theta_2 + \ddot{\theta}_3 + \left(1 - 2\frac{\bar{\lambda}}{\lambda_c}\right)\theta_3 = 0 \tag{35}$$

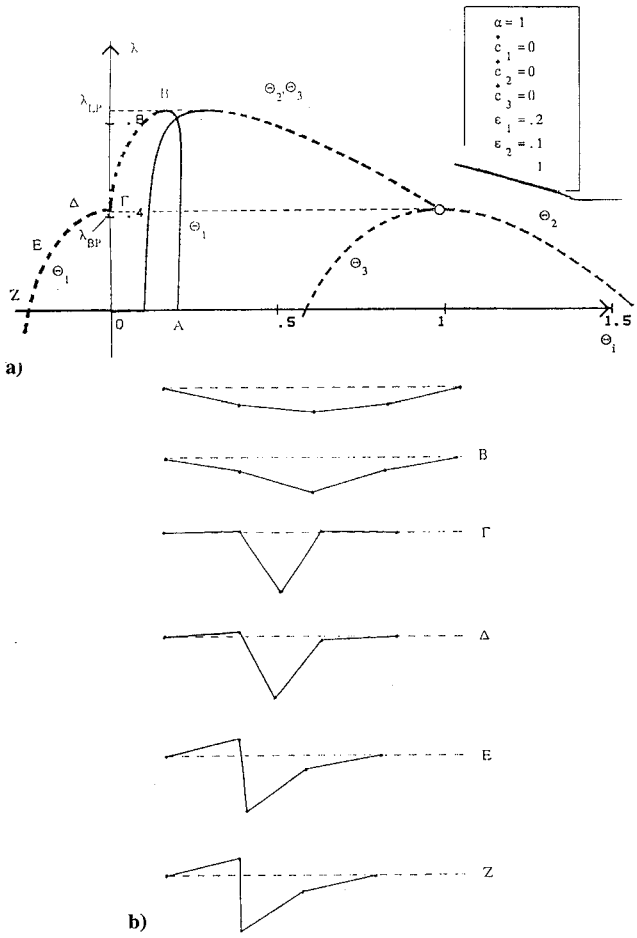

Fig. 2 Model having symmetric imperfections with $\bar{a} \leq 1.3$: a) nonlinear equilibrium paths with postlimit point bifurcation and b) corresponding deformed configurations.

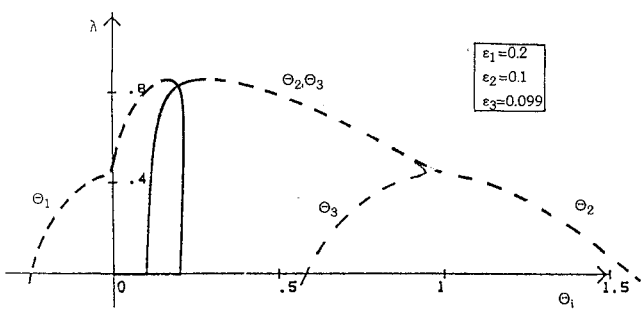

Fig. 3 Nonlinear equilibrium paths for model having nearly symmetric imperfections with $\bar{a} \leq 1.3$.

Setting

$$\theta_1 = \bar{\theta}_1\cdot e^{i\omega t} \Rightarrow \ddot{\theta}_1 = -\omega^2\cdot\bar{\theta}_1\cdot e^{i\omega t}$$
$$\theta_2 = \bar{\theta}_2\cdot e^{i\omega t} \Rightarrow \ddot{\theta}_2 = -\omega^2\cdot\bar{\theta}_2\cdot e^{i\omega t} \tag{36}$$
$$\theta_3 = \bar{\theta}_3\cdot e^{i\omega t} \Rightarrow \ddot{\theta}_3 = -\omega^2\cdot\bar{\theta}_3\cdot e^{i\omega t}$$

and then substituting Eq. (36) into Eqs. (33–35), we can obtain the

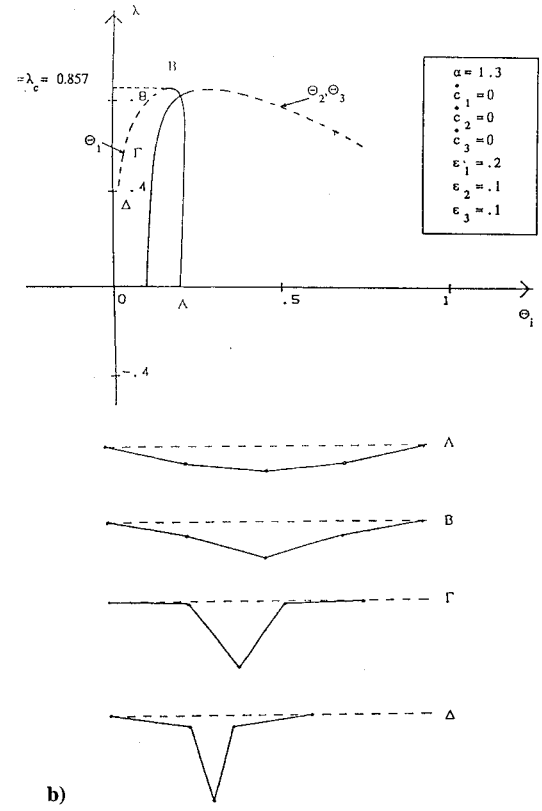

Fig. 4 Model having symmetric imperfections with $\bar{a} \geq 1.3$: a) nonlinear equilibrium paths without postlimit point bifurcation and b) corresponding deformed configurations.

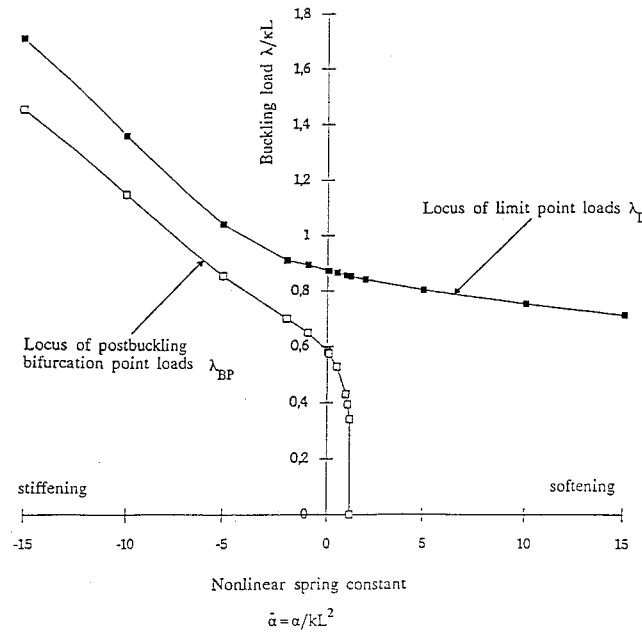

Fig. 5 Influence of the nonlinear spring constant $\bar{a}$ on the postlimit point behavior for symmetric initial imperfections.

eigenfrequencies of the model by setting the determinant of the coefficients of the system of equations equal to zero:

$$\begin{vmatrix} \left(3-2\frac{\bar{\lambda}}{\lambda_c}-3\omega^2\right) & \left(2-\frac{\bar{\lambda}}{\lambda_c}-2\omega^2\right) & \left(-1+\frac{\bar{\lambda}}{\lambda_c}+\omega^2\right) \\ \left(2-\frac{\bar{\lambda}}{\lambda_c}-2\omega^2\right) & \left(2-2\frac{\bar{\lambda}}{\lambda_c}-2\omega^2\right) & \left(-1+\frac{\bar{\lambda}}{\lambda_c}+\omega^2\right) \\ \left(-1+\frac{\bar{\lambda}}{\lambda_c}+\omega^2\right) & \left(-1+\frac{\bar{\lambda}}{\lambda_c}+\omega^2\right) & \left(1-2\frac{\bar{\lambda}}{\lambda_c}-\omega^2\right) \end{vmatrix} = 0 \tag{37}$$

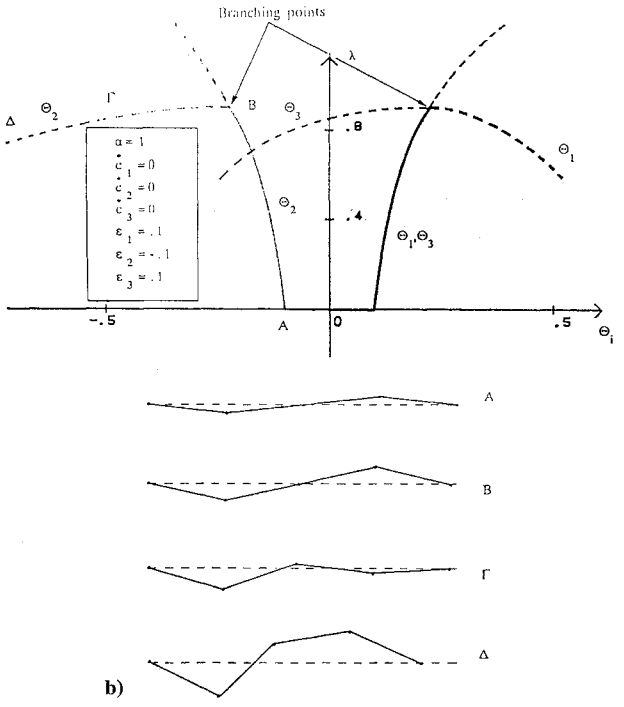

Fig. 6 Model with antisymmetric imperfections: a) nonlinear equilibrium paths with prelimit point bifurcation and b) corresponding deformed configurations.

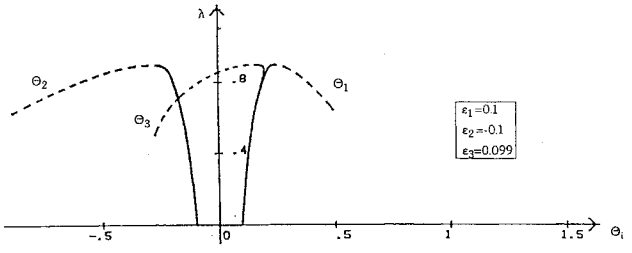

Fig. 7 Nonlinear equilibrium paths for model with nearly antisymmetric imperfections.

This leads to the algebraic equation

$$\left(1-2\frac{\bar{\lambda}}{\lambda_c}-\omega^2\right)\cdot\left\{\omega^4+\left(4\frac{\bar{\lambda}}{\lambda_c}-2\right)\omega^2+\left[1-4\frac{\bar{\lambda}}{\lambda_c}+2\left(\frac{\bar{\lambda}}{\lambda_c}\right)^2\right]\right\}=0 \tag{38}$$

with solutions

$$\begin{aligned} \omega_1^2 &= 1-(\sqrt{2}+2)(\bar{\lambda}/\lambda_c) \\ \omega_2^2 &= 1-2(\bar{\lambda}/\lambda_c) \\ \omega_3^2 &= 1+(\sqrt{2}-2)(\bar{\lambda}/\lambda_c) \end{aligned} \tag{39}$$

The fundamental frequency ω_0 of the system is the smallest of the three values ω_1, ω_2, and ω_3.

The coefficients $\bar{q}_i$ of the right-hand side of Eq. (16) correspond to the vertical displacements of the three masses m_i, measured from the initial deformed configuration. Hence,

$$\begin{aligned} \bar{q}_1 &= L\cdot(\sin\theta_1-\sin\varepsilon_1) \\ \bar{q}_2 &= L\cdot(\sin\theta_1+\sin\theta_2-\sin\varepsilon_1-\sin\varepsilon_2) \\ \bar{q}_3 &= L\cdot(\sin\theta_1+\sin\theta_2-\sin\theta_3-\sin\varepsilon_1-\sin\varepsilon_2+\sin\varepsilon_3) \end{aligned} \tag{40}$$

Then Eq. (16) becomes

$$\begin{aligned} V_T \le -\left(L^2\cdot\omega_0/\pi\right)\cdot\{&c_1\cdot(\sin\theta_1-\sin\varepsilon_1) \\ &+c_2\cdot(\sin\theta_1+\sin\theta_2-\sin\varepsilon_1-\sin\varepsilon_2) \\ &+c_3\cdot(\sin\theta_1+\sin\theta_2-\sin\theta_3-\sin\varepsilon_1-\sin\varepsilon_2+\sin\varepsilon_3)\} \end{aligned} \tag{41}$$

IV. Numerical Results

Figure 2a illustrates the static equilibrium paths for a model with symmetric initial goemetric imperfections. The corresponding deformed configurations are shown in Fig. 2b. The behavior is characterized by a postlimit point bifurcation (point Γ). After that point the deformation of the model stops being symmetric. If the initial imperfections deviate slightly from the completely symmetric configuration, then the static equilibrium paths are as illustrated in Fig. 3. The postlimit point bifurcation and the loss of symmetry of the deformed configuration do not take place for stiffer springs, as illustrated in Fig. 4. The influence of the nonlinear spring component [i.e., $\bar{a} = a/(k\cdot L^2)$] is demonstrated in the plot of Fig. 5. It can be observed that for the specific example the smallest difference between limit point load λ_S and postbuckling bifurcation point load λ_C occurs for $\bar{a} = -5$ (soft spring), whereas no bifurcation takes place for $\bar{a} \ge 1.3$. Note that for a model of this type with three bars, the branching point appears prior to the limit point.[4]

Figure 6 shows equilibrium paths and corresponding successive deformed configurations for a model with antisymmetric geometric imperfections. The behavior is characterized by a prelimit point bifurcation after which the deformed shape stops being antisymmetric. The corresponding plot for a nearly antisymmetric system is shown in Fig. 7.

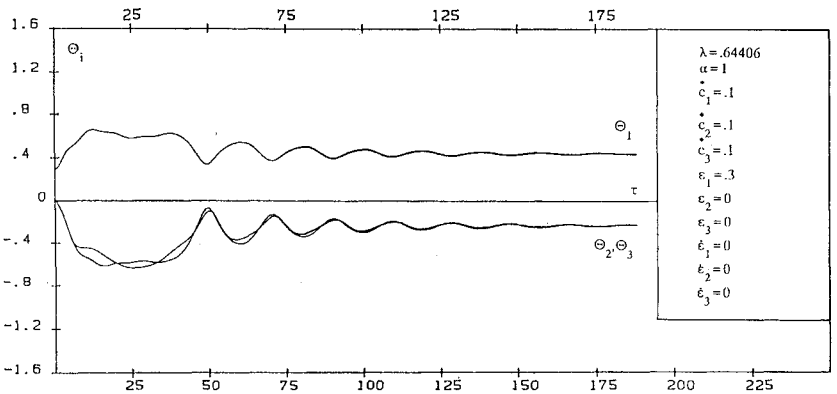

Fig. 8 Times series $\mathcal{I}_i, i = 1, 2, 3$ vs τ for a dissipative symmetric model showing a point attractor response (stable motion) for $\lambda = 0.644060 < \lambda_{DD} = 0.644065$, where λ and λ_{DD} have been divided by λ_C.

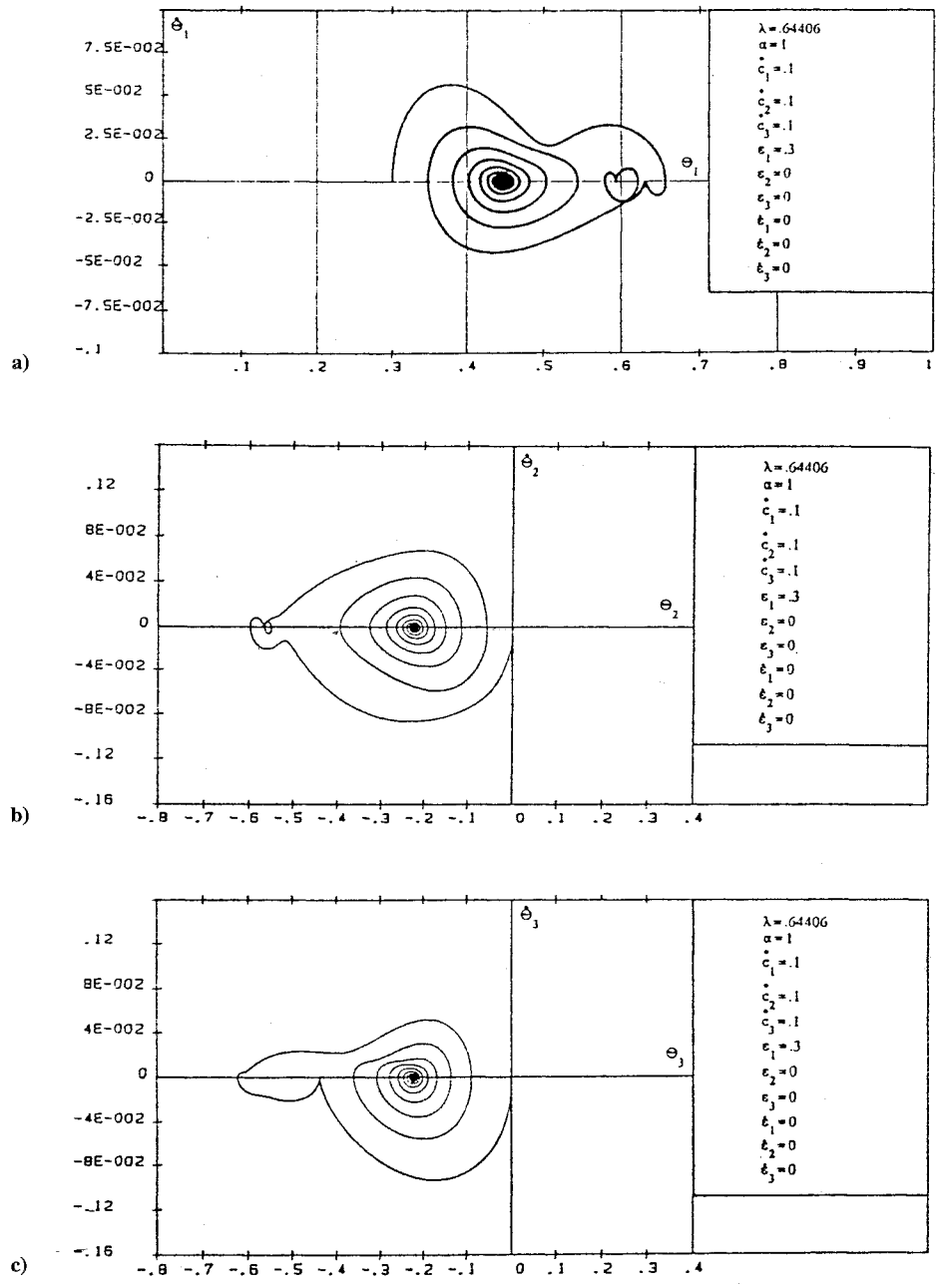

Fig. 9 Point attractor response for a dissipative symmetric model with $\lambda = 0.644060 < \lambda_{DD} = 0.644065$ shown in three-phase plane portraits $(\theta_i, \dot{\theta}_i)$ with $i = 1, 2, 3$.

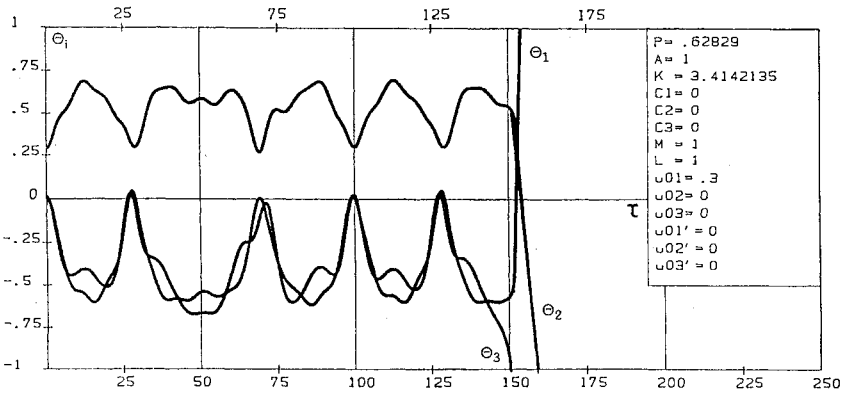

Fig. 10 Time series: $\mathcal{I}_i$, $i = 1, 2, 3$ vs τ for a dissipative symmetric model showing dynamic buckling (escaped motion) for $\lambda = 0.644070 > \lambda_{DD} = 0.644065$.

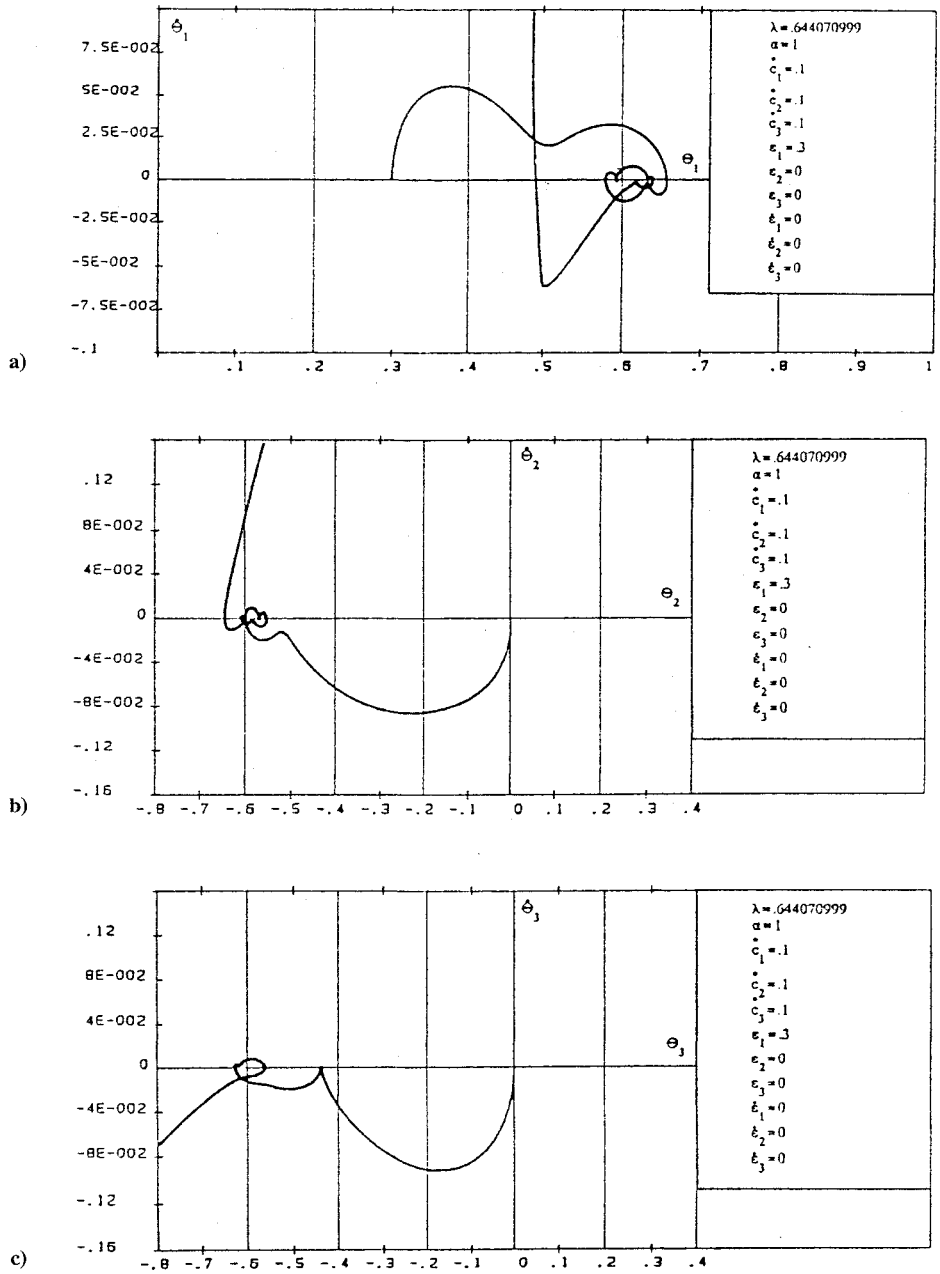

Fig. 11 Dynamic buckling (escaped motion) for a dissipative symmetric model with $\lambda = 0.644070 > \lambda_{DD} = 0.644065$ shown in three-phase plane portraits $(\theta_i, \dot{\theta}_i)$ with $i = 1, 2, 3$.

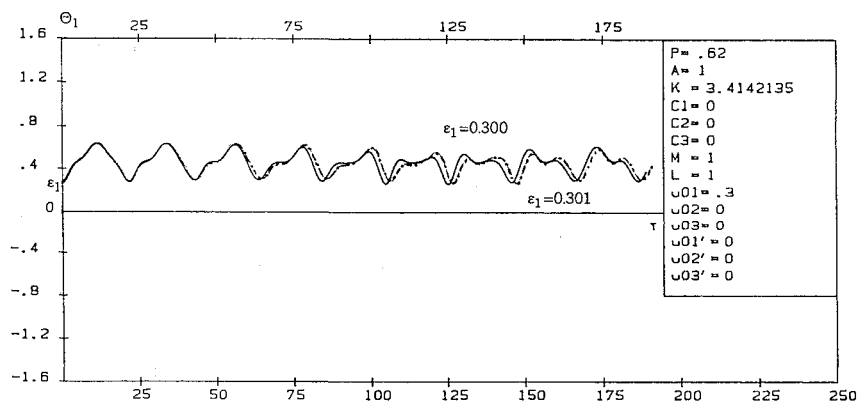

Fig. 12 Divergence from two adjacent initial configurations corresponding to $\varepsilon_1 = 0.300$ and $\varepsilon_1 = 0.301$ for an initially symmetric model.

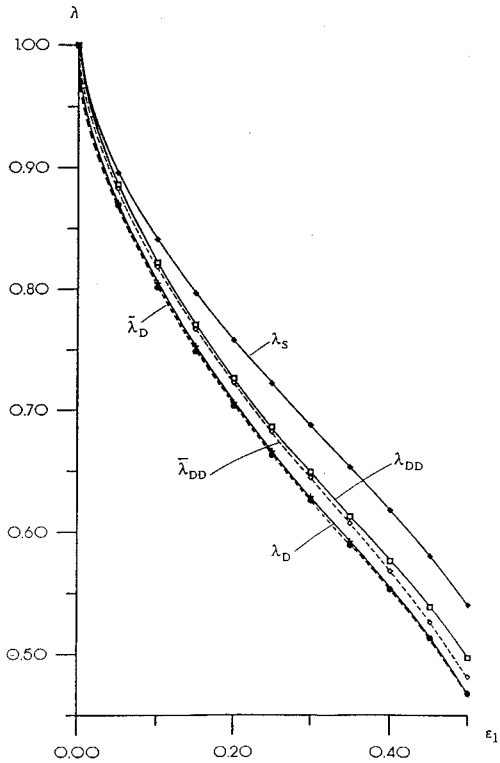

Fig. 13 Variation of the dynamic [exact λ_{DD} (with damping), λ_D (without damping), and approximate $\bar{\lambda}_{DD}$ and $\bar{\lambda}_D$ (vanishing damping)] and static buckling loads λ_C vs the initial angle ε_1 for a symmetric model.

Figure 8 shows plots of θ_1, θ_2, and θ_3, vs the time τ for a dissipative model with symmetric initial imperfections. Since the applied load is smaller than the dynamic buckling load, the resulting motion is bounded converging toward the stable equilibrium state. The corresponding phase-plane protraits are shown in Fig. 9. Figures 10 and 11 illustrate the time series plots and phase-plane portraits for the same initial conditions but slightly higher load (exceeding the dynamic buckling load), which leads to an unbounded (escaped) motion.

Figure 12 shows the divergence from two adjacent initial configurations corresponding to $\varepsilon_1 = 0.300$ and $\varepsilon_1 = 0.301$ for an initially symmetric model.

Finally, Fig. 13 illustrates the validity of Eq. (18a) for a model with symmetric initial imperfections ($\varepsilon_2 = \varepsilon_3 = 0$ and ε_1 ranging from 0 to 0.5).

V. Conclusions

In all cases considered dynamic buckling (escaped motion) occurs through a saddle point with $V \leq 0$ (Refs. 3–7). For this 3-DOF nonlinear elastic and dissipative model one may draw the following important conclusions.

Static Loading

1) The symmetric model under statically applied load exhibits a postlimit point bifurcation which breaks the symmetry of the deformed configuration. If this model has three bars (instead of four) the branching point occurs prior to limit point.

2) The effect of the spring cubic soft type material nonlinearity on the nonlinear equilibrium path is discussed in detail.

3) When an initially antisymmetric model is subjected to a static load, the loss of stability takes place through an unstable branching point lying on the nonlinear equilibrium path prior to the limit point.

Dynamic Loading

1) In all cases considered, the dissipative model under a step load of infinite duration exhibits either a point attractor response for $\lambda < \lambda_{DD}$ or dynamic buckling (escaped motion) via a saddle of the unstable postbuckling equilibrium path with $V \leq 0$.

2) For a model under step loading of infinite duration with or without damping exact (for vanishing damping) and lower/upper bound dynamic buckling estimates are established. These estimates confirm previous results obtained for other types of 2-DOF models and are very useful for structural design purposes, particularly in case of large time solutions or in case of sensitivity to initial conditions or to damping.

3) For a symmetric model (with symmetric imperfections $\varepsilon_2 = \varepsilon_3 = 0$) under step load of infinite duration regardless of the variation of the initial angle ε_1, the proposed dynamic buckling estimates are very close to the exact loads.

4) The reliability, efficiency, and usefulness of the proposed readily obtained dynamic buckling estimates which allow us to avoid the integration of the highly nonlinear equations of motion is obvious.

References

[1]Kounadis, A. N., "Global Bifurcations with Chaotic and Other Stability Phenomena in Simple Structural Systems," Invited lecture in the honor of P. Theocaris, *Future Trends in Applied Mechanics*, National Technical Univ. of Athens, Greece, 1989, pp. 275–299.

[2]Kounadis, A. N., "Nonlinear Dynamic Buckling of Discrete Dissipative or Nondissipative Systems under Step Loading," *AIAA Journal*, Vol. 29, No. 2, 1991, pp. 280–288.

[3]Kounadis, A. N., "Nonlinear Dynamic Buckling and Stability of Autonomous Structural Systems," *International Journal of Mechanical Sciences*, Vol. 35, No. 8, 1993, pp. 643–656.

[4]Kounadis, A. N., Gantes, C., and Kandakis, G., "Numerical Solutions and Theoretical Predictions Based on Energy Criteria for Establishing the Dynamic Response of Autonomous Dissipative and Non-Dissipative Systems," First Greek National Congress on Computational Mechanics, Athens, Greece, Sept. 1992, pp. 601–609.

[5]Kounadis, A. N., "Static and Dynamic, Local and Global Bifurcations in Nonlinear Autonomous Structural Systems," *AIAA Journal*, Vol. 31 No. 8, 1993, pp. 1468–1477.

[6]Kounadis, A. N., "A Qualitative Analysis for the Local and Global Dynamic Buckling and Stability of Autonomous Discrete Systems," *Quarterly Journal of Mech. Appl. Math.*, Vol. 47, Pt. 2, 1994, pp. 269–296.

[7]Kounadis, A. N., "Nonlinear Dynamic Buckling and Stability of Autonomous Dissipative Discrete Structural Systems," *Proceedings*, Center International des Sciences Mécaniques, Sept. 1993, Udine, Italy (to be published).

[8]Kounadis, A. N., "An Efficient and Simple Approximate Technique for Solving Nonlinear Initial and Boundary-Value Problems," *Computational Mechanics*, Vol. 2, 1992, pp. 221–231.

[9]Kounadis, A. N., "Nonlinear Dynamic Buckling of Discrete Structural Systems under Impact Loading," *International Journal of Solids and Structures*, Vol. 30, No. 21, 1993, pp. 2895–2909.

[10]Thompson, J. M. T., and Hunt, G. W., *General Theory of Stability*, Wiley, New York, 1973, p. 102.